Cold Junction Compensation Technique of Thermocouple Thermometer Using Radiation-Hardened-by-Design Voltage Reference for Harsh Radiation Environment

Minuk Seung, Wooyoung Choi, *Member, IEEE*, Seop Hur, and Inyong Kwon

***Abstract*— This article introduces a radiation-hardened-by-design (RHBD) cold junction compensation (CJC) circuit to compensate for the voltage variation at the cold junction of a thermocouple used in a nuclear power plant (NPP) to detect the reactor temperature. The key idea of the RHBD circuit is to cancel the error induced by radiation, subtracting two reference voltages. In this design, two conditions should be satisfied to realize the first-order cancellation. First, the two voltages should have similar changes according to temperature and radiation. Therefore, two identical voltage generators are used in the proposed circuit. Second, the two reference voltages might have different values. The proposed circuit was fabricated using general purpose 0.18-μm complementary metal–oxide–semiconductor (CMOS) technology with a shallow trench isolation (STI) process. The RHBD CJC circuit showed a reference voltage of 275 mV at room temperature. The final output voltage variation was 5.2 mV under irradiation up to 2 Mrad, and the temperature coefficient (TC) was 2.9 ppm/°C in a range of 20 °–110 °C without additional trimming and annealing. The proposed circuit showed improvements of 60% and 90% for the radiation effect and temperature variation, respectively, compared with the conventional reference circuit. The active area and power consumption were 0.035 mm^2 and 1.716 mW, respectively.**

***Index Terms*— Bandgap reference (BGR) circuit, cold junction compensation (CJC) circuit, CJC, first-order cancellation, radiation hardening, radiation-hardened-by-design (RHBD) circuit, temperature sensor, total ionizing dose (TID) effect.**

Manuscript received 16 May 2022; revised 28 July 2022; accepted 28 August 2022. Date of publication 14 September 2022; date of current version 28 September 2022. This work was supported by the Basic Science Research Program through the National Research Foundation of Korea (NRF) funded by the Ministry of Science and Information and Communication Technology (MSIT) under Grant 2020M2A8A1000830 and Grant 2017M2A8A4017932. The Associate Editor coordinating the review process was Alvaro Hernandez. *(Corresponding author: Inyong Kwon.)*

Minuk Seung is with the Korea Atomic Energy Research Institute (KAERI), Daejeon 34057, South Korea, and also with the College of Electrical and Electronic Engineering, Yonsei University, Seoul 03722, South Korea (e-mail: minukseung@gmail.com).

Wooyoung Choi is with the College of Electrical and Electronic Engineering, Yonsei University, Seoul 03722, South Korea (e-mail: wchoi@yonsei.ac.kr).

Seop Hur is with the Korea Atomic Energy Research Institute, Daejeon 34057, South Korea (e-mail: shur@kaeri.re.kr).

Inyong Kwon is with the Korea Atomic Energy Research Institute (KAERI), Daejeon 34057, South Korea, and also with the Department of Nuclear and Radiation Safety, Korea University of Science and Technology (UST), Daejeon 34113, South Korea (e-mail: ikwon@ust.ac.kr).

Digital Object Identifier 10.1109/TIM.2022.3205931

I. Introduction

In NUCLEAR power plants (NPPs), various measurement instruments are used to monitor various internal environment conditions that can be critical for safety, including the temperature, pressure, and radiation dose. In particular, temperature is a major parameter that is used to monitor the state of a reactor and determine whether it is operated at the safety point. Thermocouple systems (TCSs) with excellent characteristics, such as linearity, a wide range, a low cost, stability, and durability, are widely installed in NPPs to observe the reactor temperature [1], [2], [3], [4], [5].

A thermocouple sensor is based on the Seebeck effect, which changes the voltage potential between two different metals when the temperature varies, as shown in the following equation [2], [5]:

$$V_T = S \cdot (T_H - T_C) \tag{1}$$

where S is the Seebeck coefficient, T_H is the temperature of hot junction (or measurement junction), and T_C is the temperature of cold junction. The temperature of measurement junction can be calculated based on the potential difference between the metals, where the other side is fixed at a specific value, which is known as cold junction compensation (CJC) [5], [6].

The integrated circuit (IC) can be generally used to compensate the cold junction, such as conventional complementary metal–oxide–semiconductor (CMOS) bandgap reference (BGR) circuits. The reference circuit provides a constant voltage to other circuits regardless of changing conditions, including process, supply voltage, and temperature (PVT) variations [7], [8], [9], [10].

Fig. 1 shows a thermocouple sensor system, which consists of a k-type thermocouple, which is well known as the most universal type, and an IC. The k-type thermocouple is composed of two terminals. The positive side is Chromel, and the negative side is Alumel [11]. On the negative side, a BGR for the CJC supplies a constant voltage, while the positive side is connected to an operational amplifier (OPAMP) to amplify the voltage difference. In this case, when the temperature of measurement junction is changed, the Chromel side thermoelectric is changed depending on the average rate

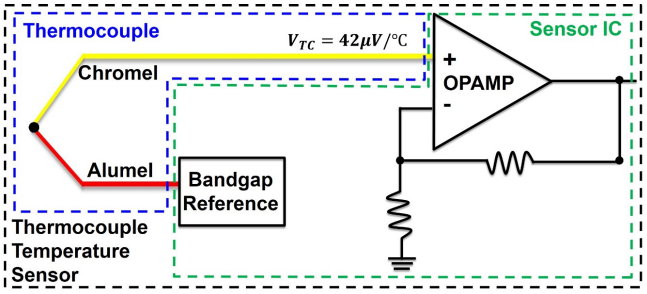

Fig. 1. TCS system block diagram with sensor IC.

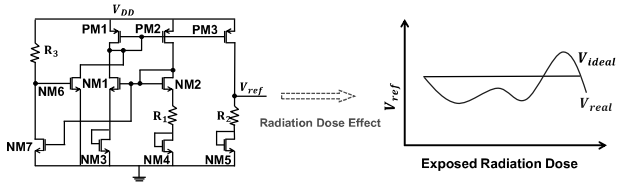

Fig. 2. Conventional voltage reference core circuit and output voltage under ideal and real conditions. Ideally, the reference voltage might be constant. However, in reality, the output voltage can vary as a result of a leakage current increase and threshold.

of 42 μV/°C that is generally known as thermal electromotive force of k-type thermocouple. An error of a few millivolts at the cold junction side can result in a temperature error of tens of degrees. For this reason, a reference voltage should supply a constant value to retain a stable output regardless of any changes in the external environments.

When the thermocouple thermometer is used in NPPs, radiation can dominantly affect to the cold junction IC. Total ionizing dose (TID) effect is well known as that it can critically degrade the performance of electronic circuit systems [12], [13]. When incident radiation penetrates the oxide region of the metal–oxide–silicon field-effect transistor (MOSFET), it generates electron–hole pairs (EHPs) [7]. Some carriers are promptly recombined or escape from the dielectric, but other carriers, especially holes, can be trapped in the SiO_2 or SiO_2–Si interface [14]. The cumulative damage causes performance degradation in CMOS devices in terms of a threshold voltage shift, leakage current increase, and noise increase [15], [16]. Therefore, ways to mitigate the TID effect should seriously be considered for the ICs in NPPs.

In the case of a CJC circuit, such as BGR, a reference voltage can be changed by the TID effect, as shown in Fig. 2. It is well known that the diodes of a BGR circuit, consisting of NM3, NM4, and NM5, are the most vulnerable devices in a BGR structure because of the leakage paths formed by radiation [9], [10].

A previous study claimed that an edgeless structure can be used to reduce the radiation effect on a MOSFET, which is called an enclosed layout transistor (ELT). The ELT does not have an edge that can cause a parasitic channel when radiation penetrates the CMOS [17]. It has already been verified that a radiation hardened structure has low sensitivity to the TID effect [7], [8], [9]. However, an ELT has some penalties related to the difficulty of design and electrical model [18]. The circuit

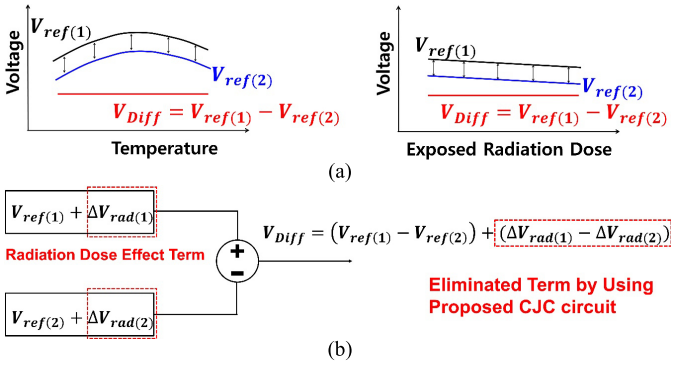

Fig. 3. Concept of the proposed CJC circuit. (a) Basic principle of radiation hardening and (b) mathematical diagram showing output voltage shift removed by subtracting temperature and radiation variations.

design could be complicated for the engineers due to the uncommon process in terms of wiring and arrangement of the transistor in the layout. In addition to the complicated design, the circuit designers could not accurately simulate the circuit behaviors because it was difficult to develop an electrical model of the ELT structure. Therefore, the reliability could be lower than that of a standard commercial CMOS process [19], [20].

Other researchers introduced radiation hardening methods without specific structures to overcome the disadvantages of the ELT using the circuit design technique called radiation hardened by design (RHBD) [21], [22], [23], [24]. This article shows how the proposed CJC circuit can be implemented without using the ELT structure but using standard MOSFETs for radiation hardening in the complementary 0.18-μm process.

II. Circuit Description

A. Strategy of Circuit Design

In this article, the first order cancellation technique is introduced by using a voltage subtracting circuit to minimize the radiation effect.

Fig. 3 shows the concept of the proposed RHBD CJC circuit. The key idea is that the voltage variation induced by the external environment can be minimized by subtracting the two voltages that have identical temperature and radiation characteristics, as shown in Fig. 3(a). Although the voltage variation is generated by radiation, as expressed as ΔV_{rad}, a final constant output can be maintained by subtracting each voltage error, as illustrated in Fig. 3(b). The detailed technique is explained in Section II-B.

B. Operation Principle

Two conditions are considered to realize the RHBD CJC circuit implementation. First, the two voltages should have similar variation patterns according to radiation and temperature as aforementioned. Thus, the voltage generation parts are identically designed in terms of the MOSFET size, structure, and resistor value to satisfy the first condition. The TID effect is depending on the circuit structure, bias, and defects on the material and so on [7], [10], [15], [16], [17]. Therefore,

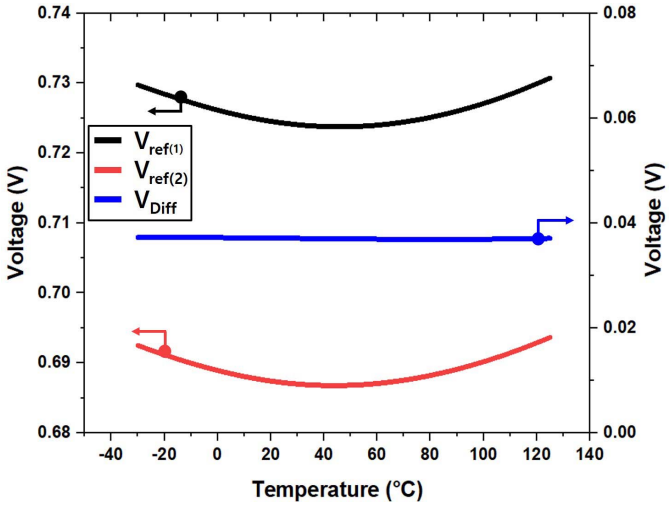

Fig. 4. Simulated output reference voltages of two voltage generators when two circuits are provided with different bias voltages. The reference voltages have similar TCs. Moreover, the difference between the two voltages is stable under various temperatures.

the identical structure might reduce the mismatch probability generated by TID effect. Second, the two voltages have different values to generate voltage difference (V_{Diff}). The voltage generator parts are biased by different voltages. Therefore, even though the voltage generators are designed identically, they can generate different output voltages.

Fig. 4 shows the results of a simulation to verify whether two conditions were feasible when supplying the two generators with different bias voltages in the range of −30 °C to +125 °C. The two voltages were 730 and 690 mV when the bias voltages of the two voltage generators were 2.8 and 1.5 V, respectively. The voltage difference (V_{Diff}) was calculated to be 38 mV. The temperature coefficients (TCs) of the voltage generators and V_{Diff} were 45 ppm/°C and 15 ppm/°C, respectively. Therefore, the method for providing the reference voltage using different bias voltages is valid.

C. Implementation of the Proposed RHBD CJC Circuit Structure

Fig. 5 shows the proposed RHBD CJC circuit architecture consisting of two identical voltage generators with two source follower buffers and a voltage subtracting circuit. As aforementioned, two voltage generator circuits are designed identical specification in terms of MOSFET and resistor size. The differentiating mark is used to prevent to confuse in the subsequential equation derivation. All the bias voltages are provided by using external equipment, whereas the reference voltages are generated by reference circuit in this article. Table I shows the specifications of the OPAMP for voltage subtractor, which generates the final output voltage in the proposed circuit. These properties were simulated after extraction of parasitic capacitance and resistance.

Two generator circuits are supplied with different bias voltages, V_{bias1} and V_{bias2}, as mentioned before. The voltage generator is designed by using the conventional BGR structure. The proportional to absolute temperature (PTAT) current is

TABLE I
SPECIFICATIONS OF DIFFERENTIAL AMPLIFIER FOR SUBTRACTING

Design parameter	Value
Open loop gain	72.5 dB
Phase margin	56.5°
Power consumption	750 uW
Supply voltage	3.3 V
Gain bandwidth product	48 MHz
Miller capacitance	500 fF
Input impedance	87 kohm
Output impedance	2.4 kohm

obtained by the ratio of the diodes, NM3 and NM4. The current mirror, consisting of PM1, PM2, and PM3, can provide the PTAT current to R_2 and NM5. The PTAT current in a conventional BGR is expressed in the following equation [26]:

$$I_{\text{PTAT}} = \frac{V_{R_1}}{R_1}. \tag{2}$$

The PTAT voltage generated across resistor R_2 is expressed in the following equation:

$$V_{\text{PTAT}} = \frac{R_2}{R_1} V_{R_1}. \tag{3}$$

In addition, the complementary to absolute temperature (CTAT) voltage of NM5 (V_{NM5}), which is decreased by temperature, can cancel out the temperature change in the circuit system. Consequently, the total reference voltage is simplified as follows:

$$V_{\text{ref}} = \frac{R_2}{R_1} V_{R_1} + V_{\text{NM5}}. \tag{4}$$

The voltage shift induced by radiation is added to the following equation and expressed as ΔV_{rad}:

$$V_{\text{ref}} = \frac{R_2}{R_1} V_{R_1} + V_{\text{NM5}} + \Delta V_{\text{rad}}. \tag{5}$$

As previously mentioned, the two voltage generators have different bias voltages to generate a difference between the two reference voltages. The reference current ($I_{\text{ref}} = I_{\text{PTAT}}$) decreases in the BGR provided a lower bias voltage. Moreover, the low current causes a decrease in the CTAT voltage applied at the MOSFET diode. Therefore, the reference voltages of the two BGR circuits have different values, as expressed in the following equations, based on (5):

$$V_{\text{ref}(1)} = \frac{R_2}{R_1} V_{R_1} + V_{\text{NM5}} + \Delta V_{\text{rad}} \tag{6}$$

$$V_{\text{ref}(2)} = \frac{R_{2'}}{R_{1'}} V_{R_{1'}} + V_{\text{NM5}'} + \Delta V_{\text{rad}'}. \tag{7}$$

By simple subtraction, the difference between the two reference voltages is defined by the following equation:

$$\begin{aligned} V_{\text{Diff}} &= V_{\text{ref}(1)} - V_{\text{ref}(2)} \\ &= \frac{R_2}{R_1}(V_{R_1} - V_{R_1'}) + (V_{\text{NM5}} - V_{\text{NM5}'}) \\ &\quad + (\Delta V_{\text{rad}} - \Delta V_{\text{rad}'}). \end{aligned} \tag{8}$$

The subtracting circuit consists of a traditional two-stage OPAMP and four resistors. According to the OPAMP feedback

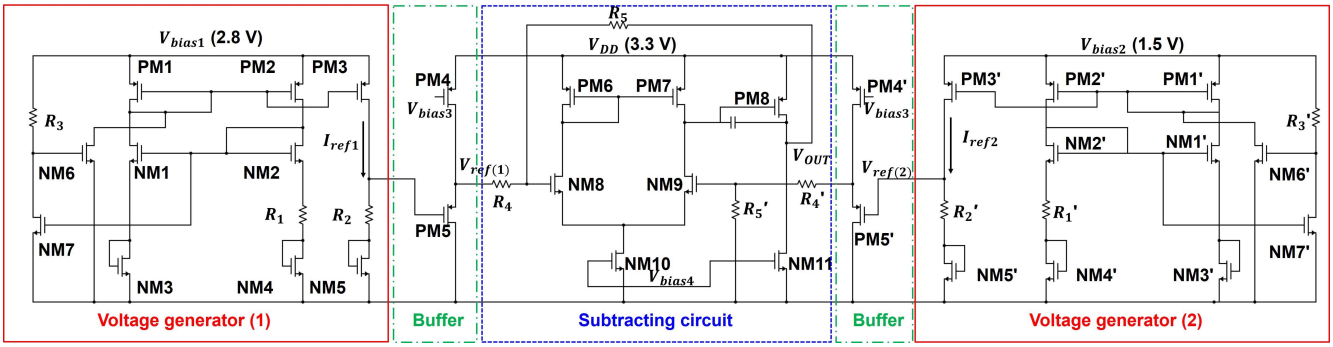

Fig. 5. Architecture of the proposed RHBD CJC circuit block diagram and detailed schematic.

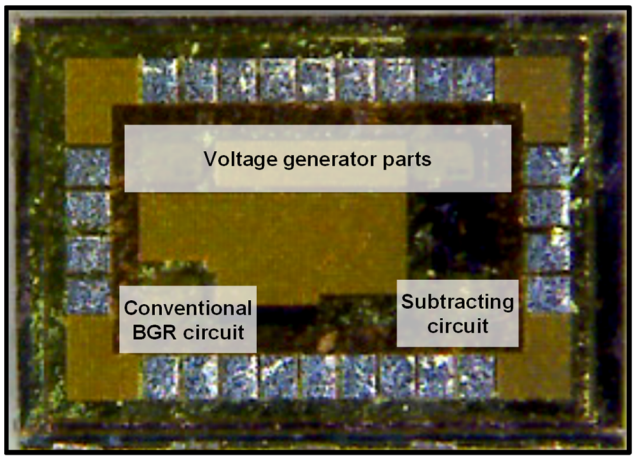

Fig. 6. Photograph of the proposed RHBD CJC circuit and conventional BGR.

loop system, the final output value of the subtracting circuit is determined by the resistor ratio, which is described as follows:

$$V_{\text{out}} = \frac{R_5}{R_4}\left[\frac{R_2}{R_1}(V_{R_1} - V_{R_{1'}}) + (V_{\text{NM5}} - V_{\text{NM5}'}) + (\Delta V_{\text{rad}} - \Delta V_{\text{rad}'})\right]. \quad (9)$$

III. Experiment Result

A chip die photograph is shown in Fig. 6. The RHBD CJC circuit was fabricated using a 0.18-μm general purpose shallow trench isolation (STI) process. The chip had one proposed CJC circuit and one conventional BGR circuit to compare the performance. The chip's active areas were 0.035 mm^2 for the proposed CJC and 0.012 mm^2 for the conventional BGR. The proposed circuit provided a final reference voltage of 275 mV when two voltage generators in the RHBD CJC were supplied with different bias voltages: 2.8 and 1.5 V. The conventional BGR circuit output was 730 mV at room temperature when a bias voltage of 2.8 V was applied.

In this study, three types of experiments were conducted: irradiation, temperature, and thermocouple operation tests. Fig. 7 shows the irradiation test environment and results. The

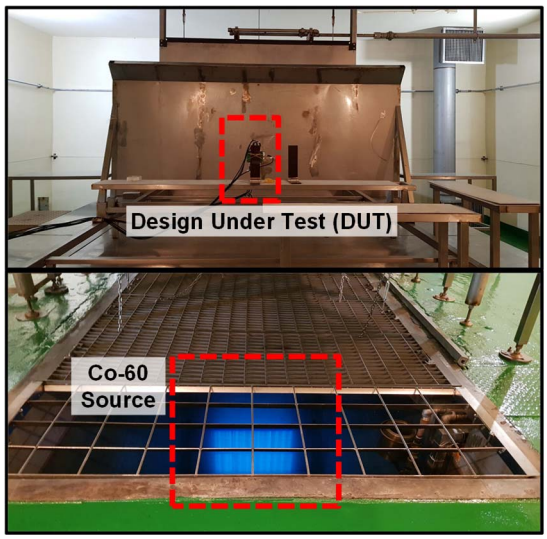

(a)

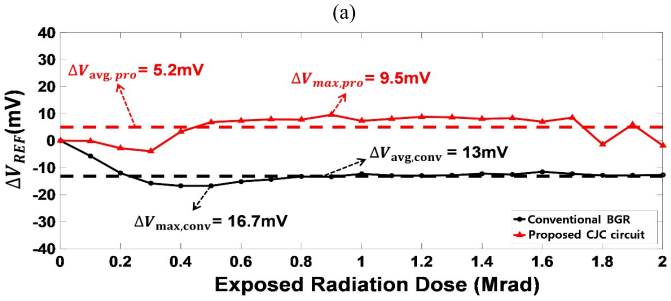

(b)

Fig. 7. (a) Irradiation facility for radiation experiment and (b) output reference voltage changes of the conventional and proposed CJC circuits versus irradiation dose.

Cobalt-60 gamma ray source at the Korea Atomic Energy Research Institute (KAERI) was used for the irradiation test, with a high-level activity of 490 kCi. The testing board was exposed to up to 2 Mrad (SiO_2) at a rate of 100 krad per hour.

The design under test (DUT) board was placed at a distance of 1 m from the radiation source [see Fig. 7(a), top]. The radiation source was placed underwater to shield the radiation during the setup of the experimental equipment [see Fig. 7(a), bottom] and then raised to the surface when the experiment began. Fig. 7(b) presents the test results, showing that the

TABLE II
COMPARISON OF PERFORMANCE WITH THOSE OF OTHER RADIATION HARDENED BGR CIRCUITS

parameter	This Work		[7]	[8]	[9]	[10]
	Conventional	Proposed				
Technology	Complementary 180 nm		130 nm ELT	180 nm ELT	65 nm ELT	130 nm
Temperature Range (°C)	20 – 110		37.5 – 100	-25 – 125	-40 – 80	-40 – 125
Power Consumption	414 μW	1.716 mW	N/A	240 μW	570 μW	N/A
Supply Voltage (V)	2.8	3.3	N/A	1.2	5	1.5
Reference Voltage (V)	0.736	0.275	0.527	0.33	1	0.6
Temperature Coefficient (ppm/°C)	289	2.9	9.1	130	141	15
ΔV_{rad} (due to the radiation)	13 mV @2 Mrad	5.2 mV @2 Mrad	6 mV @1 Mrad	33 mV @800 Mrad	5.4 mV @300 krad	18 mV @4.5 Mrad
Die size (mm^2)	0.012	0.035	N/A	0.018	0.035	0.7

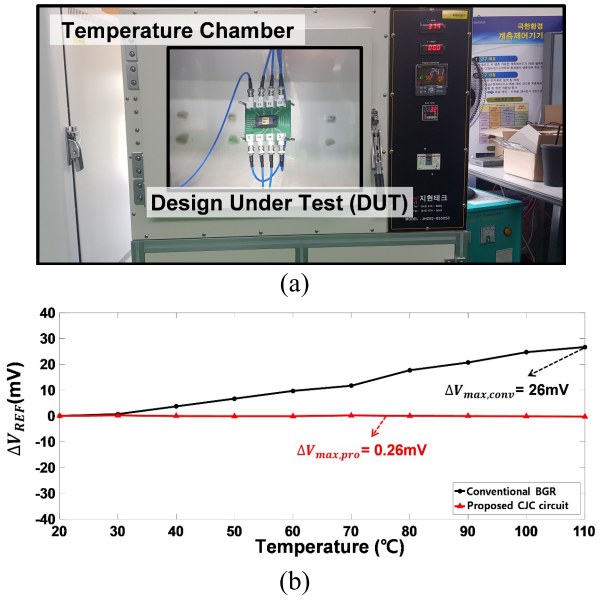

Fig. 8. (a) Temperature experiment environment and (b) output reference voltage changes of the conventional and proposed CJC circuits versus temperature.

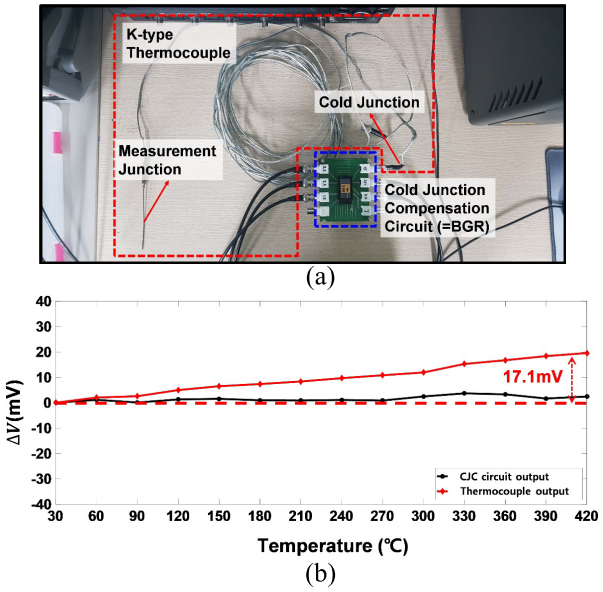

Fig. 9. Operation test of CJC. (a) *K*-type thermocouple is coupled with the RHBD CJC circuit at the negative lead. The positive lead is connected to an oscilloscope to observe the change in the output. (b) Output reference voltage changes with the thermocouple output and proposed CJC circuit versus temperature.

proposed RHBD design had a maximum radiation error of 9.5 mV and an average error of 5.2 mV, whereas the conventional BGR had 16.7 and 13 mV, respectively. The radiation sensitivity improved by 43% for the maximum error and 60% for the average error.

The temperature experiment was conducted at a rate of 1 °C/min from 20 °C to 110 °C in a temperature chamber, as displayed in Fig. 8(a). The test result is shown in Fig. 8(b). The maximum voltage variation of the proposed design was 0.26 mV, while that of the conventional circuit was 26 mV, and the TCs were 2.9 ppm/°C and 289 ppm/°C, respectively.

The test results showed that the proposed RHBD CJC circuit output a relatively constant voltage with irradiation dose and temperature increases without calibration, while the traditional reference circuit was not compensated. Therefore, the proposed reference circuit was less susceptible than the conventional BGR.

Fig. 9 shows the experiment result and test environment of the proposed CJC circuit coupled to a thermocouple for a temperature range of 30°–420 °C. The negative lead was

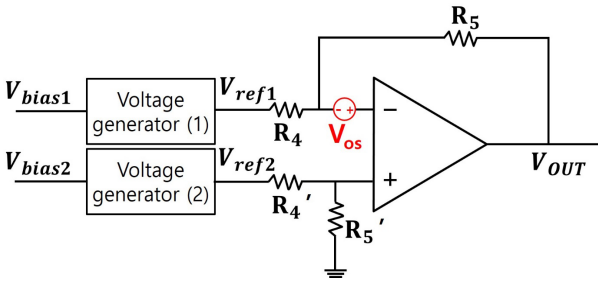

Fig. 10. Effect of the OPAMP offset on the RHBD CJC circuit. Offset source is in front of the negative port of the OPAMP.

connected to the RHBD circuit, while the output voltage of the positive lead was recorded for 2 min whenever the temperature of the measurement junction increased by 30 °C. The output voltage was expected to increase with the temperature of the measurement junction, as shown in Fig. 9(a). As seen in the

test result of Fig. 9(b), the thermocouple output was 274.3 mV at 30 °C and 291.4 mV at 420 °C. The total voltage shift was 17.1 mV, and the thermal electromotive force was calculated to be 43.8 μV/°C for a temperature change of 390 °C. This verified that the proposed circuit could be used as a CJC circuit with the proper linearity for a thermocouple.

Table II shows a comparison of the performance measurements of the proposed RHBD circuit. This work achieved relatively low variation with the radiation effects, with a good TC without calibration and an ELT structure. The power consumption was measured higher than other reference circuits because the entire design contains additional circuits, such as subtractor, two reference circuits, and buffers, requiring higher power. Since the power is provided by the external equipment, the power consumption is not a critical property in this work for NPPs.

IV. Discussion of Mismatch

This section analyzes two mismatch types. The first is between the two voltage changes due to the radiation. The RHBD CJC circuit is based on an assumption that the radiation effects on the two voltage generators are identical. Although two identical voltage reference cores are used to minimize the radiation effect in the proposed circuit, the TID effects are not identical for several reasons, such as the bias voltage, probability of EHP generation, and electric field strength as aforementioned. The PTAT current level initially changes unpredictably during the accumulation of radiation in the circuit. The initial fluctuation of a reference voltage may produce different behaviors in the voltage generators, but these changes will appear in identical directions, increasing the leakage current over time. Therefore, in environments where the chip is continuously exposed to radiation, such as NPPs and space, a radiation effect mismatch may not have a critical impact on the OPAMP input.

Second, the process mismatch is discussed. Generally, the reference circuit would need to be trimmed by controlling resistor R_2 to minimize the temperature variation because a mismatch can occur during the fabrication. Although the reference voltage varies as a result of the mismatch effect, the two voltage generators could generate a constant voltage if they have identical mismatches in the proposed schematic. Therefore, the BGRs are not required to calibrate for the mismatch, which is minimized in the proposed circuit, compared with the conventional circuit. As verified in the temperature experiment, while the conventional design dose not compensate the reference voltage, whereas the proposed CJC circuit provided a stable voltage with the temperature change.

In terms of subtracting circuit, the OPAMP has an offset voltage at the input port. Fig. 10 shows the offset in the proposed RHBD CJC circuit. The errors cause the variation of the output as expressed in the following equation:

$$V_{\text{out,OS}} = \left(1 + \frac{R_5}{R_4}\right) V_{\text{OS}}. \tag{10}$$

By using superposition, the output voltage of the proposed CJC circuit is defined in the following equation:

$$V_{\text{out}} = \frac{R_5}{R_4}\left[\frac{R_2}{R_1}(V_{R_1} - V_{R_{1'}}) + (V_{\text{NM5}} - V_{\text{NM5}'}) + (\Delta V_{\text{rad}} - \Delta V_{\text{rad}'}) + V_{\text{OS}}\right] + V_{\text{OS}}. \tag{11}$$

Therefore, if R_1 and R_2 ratio is larger than R_4 and R_5 ratio, offset will be reduced.

V. Conclusion

The radiation hardened CJC circuit was implemented using the 0.18-μm STI process without a specific device to mitigate radiation effects. The TID effect is considered as noise term in voltage form in this article. To minimize the radiation effect, the circuit exploits the first-order cancellation technique, which subtracts the outputs of two voltage generators. These circuits are supplied by different bias voltages to generate different reference voltages. By subtracting the two reference voltages, the RHBD CJC circuit can provide a constant voltage regardless of radiation and temperature variations.

The proposed CJC circuit achieves an average radiation error of 5.2 mV and a TC of 2.9 ppm/°C in the range of 20°–110 °C, while the conventional bandgap circuit had values of 13 mV and 289 ppm/°C, respectively. Therefore, the proposed circuit showed improvements of 60% and 90% for radiation and temperature variations compared to the conventional BGR, respectively.

The subtractive solution is simple, but it is effective to cancel out the radiation effects in the circuit level. It was also verified that the design could be utilized for the CJC of a thermocouple temperature sensor in radiation environments.

References

[1] G. Mei, Y. Tong, Y. Zhang, and Y. Ma, "A sensor of blackbody cavity with transparent wall for rapidly measuring the liquid temperature," *IEEE Trans. Instrum. Meas.*, vol. 69, no. 1, pp. 21–23, Jan. 2020, doi: 10.1109/TIM.2019.2954647.

[2] K. Srinivasan and P. D. Sarawade, "An included angle-based multilinear model technique for thermocouple linearization," *IEEE Trans. Instrum. Meas.*, vol. 69, no. 7, pp. 4412–4424, Jul. 2020, doi: 10.1109/TIM.2019.2947951.

[3] S. Mandal, B. Santhi, S. Sridhar, K. Vinolia, and P. Swaminathan, "Nuclear power plant thermocouple sensor-fault detection and classification using deep learning and generalized likelihood ratio test," *IEEE Trans. Nucl. Sci.*, vol. 64, no. 6, pp. 1526–1534, Jun. 2017.

[4] F. Ali and L. Lu, "A method to eliminate the effect of radiation on thermocouple performance," *Nucl. Eng. Des.*, vol. 237, no. 14, pp. 1522–1525, Aug. 2007.

[5] D. A. Lampasi and L. Podesta, "A measurement system exploiting nonlinearity of thermocouples for cold junction compensation," in *Proc. 21st IEEE Instrum. Meas. Technol. Conf.*, vol. 3, May 2004, pp. 2170–2175, doi: 10.1109/IMTC.2004.1351520.

[6] D. Hudoklin, J. Drnovsek, I. Pusnik, and J. Bojkovski, "Simultaneous calibration of a large number of thermocouples," *IEEE Trans. Instrum. Meas.*, vol. 51, no. 5, pp. 1015–1018, Oct. 2002, doi: 10.1109/TIM.2002.806009.

[7] V. Gromov, A. J. Annema, R. Kluit, J. L. Visschers, and P. Timmer, "A radiation hard bandgap reference circuit in a standard 0.13 μm CMOS technology," *IEEE Trans. Nucl. Sci.*, vol. 54, no. 6, pp. 2727–2733, Dec. 2007.

[8] B. M. McCue *et al.*, "A wide temperature, radiation tolerant, CMOS-compatible precision voltage reference for extreme radiation environment instrumentation systems," *IEEE Trans. Nucl. Sci.*, vol. 60, no. 3, pp. 2272–2279, Jun. 2013.
[9] T. Vergine, M. De Matteis, S. Michelis, G. Traversi, F. De Canio, and A. Baschirotto, "A 65 nm rad-hard bandgap voltage reference for LHC environment," *IEEE Trans. Nucl. Sci.*, vol. 63, no. 3, pp. 1762–1767, Jun. 2016.
[10] Y. Cao, W. D. Cock, M. Steyaert, and P. Leroux, "A 4.5 MGy TID-tolerant CMOS bandgap reference circuit using a dynamic base leakage compensation technique," *IEEE Trans. Nucl. Sci.*, vol. 60, no. 4, pp. 2819–2824, Aug. 2013.
[11] M. D. Bethea and B. N. Rosenthal, "An automated thermocouple calibration system," *IEEE Trans. Instrum. Meas.*, vol. 41, no. 5, pp. 702–706, Oct. 1992, doi: 10.1109/19.177346.
[12] K. Ma *et al.*, "Radiation-induced degradation analysis and reliability modeling of COTS ADCs for space-borne miniature fiber-optic gyroscopes," *IEEE Trans. Instrum. Meas.*, vol. 70, pp. 1–8, 2021, doi: 10.1109/TIM.2021.3054419.
[13] B. V. Bockel, P. Leroux, and J. Prinzie, "Tradeoffs in time-to-digital converter architectures for harsh radiation environments," *IEEE Trans. Instrum. Meas.*, vol. 70, pp. 1–10, 2021, doi: 10.1109/TIM.2021.3100355.
[14] J. D. Cressler and H. A. Mantooth, "Interaction of radiation with semiconductor devices," in *Extreme Environment Electronics*, 1st ed. Boca Raton, FL, USA: CRC Press, 2013, pp. 84–88.
[15] H. J. Barnaby, "Total-ionizing-dose effects in modern CMOS technologies," *IEEE Trans. Nucl. Sci.*, vol. 53, no. 6, pp. 3103–3121, Dec. 2006.
[16] M. Manghisoni, L. Ratti, V. Re, V. Speziali, G. Traversi, and A. Candelori, "Comparison of Ionizing radiation effects in 0.18 and 0.25 μm CMOS technologies for analog applications," *IEEE Trans. Nucl. Sci.*, vol. 50, no. 6, pp. 1827–1833, Dec. 2003.
[17] W. J. Snoeys, T. A. P. Gutierrez, and G. Anelli, "A new NMOS layout structure for radiation tolerance," *IEEE Trans. Nucl. Sci.*, vol. 49, no. 4, pp. 1829–1833, Aug. 2002.
[18] H. Jeon, I. Kwon, and M. Je, "Radiation-hardened sensor interface circuit for monitoring severe accidents in nuclear power plants," *IEEE Trans. Nucl. Sci.*, vol. 67, no. 7, pp. 1738–1745, Jul. 2020.
[19] V. Re, M. Manghisoni, L. Ratti, V. Speziali, and G. Traversi, "Total ionizing dose effects on the noise performances of a 0.13 μm CMOS technology," *IEEE Trans. Nucl. Sci.*, vol. 53, no. 3, pp. 1599–1606, Jun. 2006.
[20] R. C. Lacoe, "Improving integrated circuit performance through the application of hardness-by-design methodology," *IEEE Trans. Nucl. Sci.*, vol. 55, no. 4, pp. 1903–1925, Aug. 2008.
[21] C. Lee, G. Cho, T. Unruh, S. Hur, and I. Kwon, "Integrated circuit design for radiation-hardened charge-sensitive amplifier survived up to 2 Mrad," *Sensors*, vol. 20, no. 10, p. 2765, May 2020.
[22] S. Kim, J. Lee, I. Kwon, and D. Jeon, "TID-tolerant inverter designs for radiation-hardened digital systems," *Nucl. Instrum. Methods Phys. Res. A, Accel. Spectrom. Detect. Assoc. Equip.*, vol. 954, Feb. 2020, Art. no. 161473.
[23] K. J. Shetler *et al.*, "Radiation hardening of voltage references using chopper stabilization," *IEEE Trans. Nucl. Sci.*, vol. 62, no. 6, pp. 3064–3071, Dec. 2015.
[24] H. Banba *et al.*, "A CMOS bandgap reference circuit with sub-1-V operation," *IEEE J. Solid-State Circuits*, vol. 34, no. 5, pp. 670–674, May 1999.

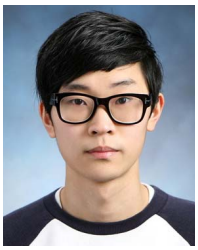

Minuk Seung received the B.S. degree in nuclear engineering from Kyunghee University, Yongin, South Korea, in 2019, and the M.S. degree in electrical engineering from Yonsei University, Seoul, South Korea, in 2021, where he is currently pursuing the Ph.D. degree in electrical engineering.

Since 2019, he has been with the Korea Atomic Energy Research Institute (KAERI), Daejeon, South Korea. His current research interests include the radiation hardened design of analog/mixed signal for the radiation detecting system.

Wooyoung Choi (Member, IEEE) received the B.S., M.S., and Ph.D. degrees in electrical engineering and computer science from the Massachusetts Institute of Technology, Cambridge, MA, USA, in 1986, 1988, and 1994, respectively.

From 1994 to 1995, he was a Post-Doctoral Research Fellow with the NTT Opto-Electronics Laboratories, Tokyo, Japan. In 1995, he joined the Department of Electrical and Electronic Engineering, Yonsei University, Seoul, South Korea, where he is currently a Professor. His current research interests include high-speed circuits and systems that include high-speed electronic circuits, optoelectronics, and optical interconnects.

Seop Hur received the B.S. and M.S. degrees in physics from Sogang University, Seoul, South Korea, in 1988 and 1990, respectively, and the Ph.D. degree in electronics from Chungnam National University, Daejeon, South Korea, in 2009.

In 1990, he joined the Korea Atomic Energy Research Institute (KAERI), Daejeon. His current research interests include radiation detector development for reactor core monitoring during severe accident.

Inyong Kwon received the B.S. degree in electrical engineering from Yonsei University, Seoul, South Korea, in 2010, and the M.S. and Ph.D. degrees in electrical engineering and computer science from the University of Michigan, Ann Arbor, MI, USA, in 2012 and 2015, respectively.

He was a Post-Doctoral Research Fellow with Stanford University, Stanford, CA, USA, in 2016. He was with the Korea Atomic Energy Research Institute (KAERI), Daejeon, South Korea. In 2021, he was also appointed as an Associate Professor of the Nuclear and Radiation Safety Department, University of Science and Technology (UST), Daejeon. His current research interests include integrated circuit (IC) design for radiation sensing and hardening that can be used in extreme and specific environments, such as nuclear power plants, space, and advanced medical instruments.